Jurnal Teknologi

Full Paper

MULTI-OBJECTIVE OPTIMIZATION OF FDM: INTEGRATING ANN AND MOSOS-DS FOR IMPROVED MATERIAL CONSUMPTION, TENSILE STRENGTH, AND DIMENSIONAL ACCURACY

Hani Nasuha Hadi Irazman[a], Mohd Sazli Saad[b]*, Mohamad Ezral Baharudin[a], Mohd Zakimi Zakaria[a], Azuwir Mohd Nor[a], Azlan Mohd Zain[a]

[a]Faculty of Mechanical Engineering Technology, Universiti Malaysia Perlis, Pauh Putra Campus, 02600 Arau, Perlis, Malaysia
[b]Faculty of Computing, Universiti Teknologi Malaysia, 81310 UTM Johor Bahru, Johor, Malaysia

Article history
Received
20 January 2025
Received in revised form
2 July 2025
Accepted
3 July 2025
Published Online
30 April 2026

*Corresponding author
sazlisaad@unimap.edu.my

Graphical abstract

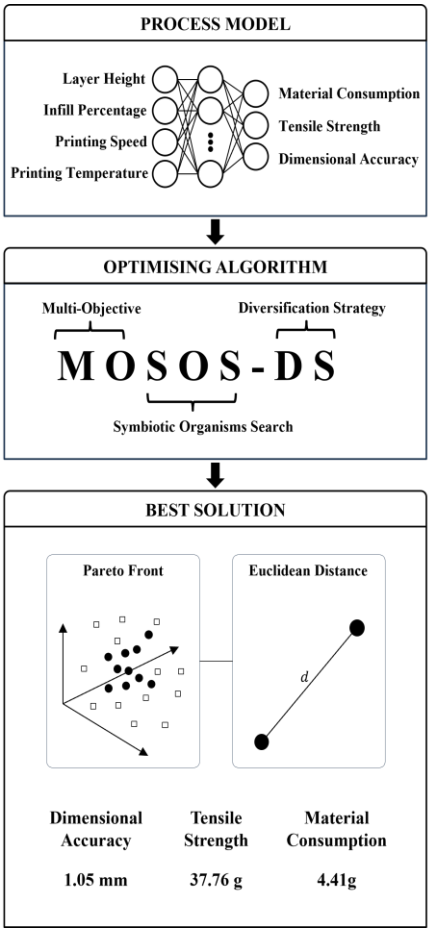

Abstract

Data-driven modelling and metaheuristic algorithms offer powerful tools for navigating the complexity of fused deposition modelling (FDM) process optimization. This study presents an integrated approach that addresses the nonlinear relationships among key input parameters, including layer height, infill density, printing temperature, and printing speed. Conventional methods often struggle to optimize conflicting objectives such as reducing material consumption while improving tensile strength and dimensional accuracy. To overcome these limitations, Artificial Neural Networks (ANN) were used to model each response based on data from 78 PLA+ specimens fabricated using a Face-Centered Central Composite Design (FCCCD). Rather than applying a fixed model structure, the best-performing ANN architecture was identified separately for each output. The selected models demonstrated high accuracy, with R^2 values of 0.9919 for material consumption, 0.9360 for tensile strength, and 0.9558 for dimensional accuracy. These models were embedded into an enhanced version of the Symbiotic Organism Search (SOS) algorithm, which incorporated a Diversification Strategy (DS) to form MOSOS-DS. Pareto-based optimization and Euclidean distance analysis yielded the best compromise solution with 4.41 g material consumption, 37.76 Pa tensile strength, and 1.05 mm dimensional accuracy. Although the individual techniques are established, their tailored combination and response-specific implementation provide a scalable framework for precise, data-driven process control in additive manufacturing (AM).

Keywords: Multi-objective optimisation (MOO), symbiotic organism search (SOS), fused deposition modelling (FDM), artificial neural network (ANN), diversification strategy

Abstrak

Pemodelan berasaskan data dan algoritma metaheuristik menawarkan pendekatan berkesan untuk menangani kerumitan pengoptimuman proses Fused Deposition Modelling (FDM). Kajian ini membentangkan pendekatan bersepadu yang menangani hubungan tidak linear antara parameter utama seperti ketinggian lapisan, ketumpatan infill, suhu pencetakan dan kelajuan pencetakan. Kaedah konvensional sering kali gagal mengoptimumkan objektif yang bercanggah, seperti mengurangkan penggunaan bahan sambil meningkatkan

kekuatan tegangan dan ketepatan dimensi. Untuk mengatasi kekangan ini, Rangkaian Neural Tiruan (ANN) digunakan bagi memodelkan setiap tindak balas berdasarkan data daripada 78 spesimen PLA+ yang dihasilkan melalui Reka Bentuk Komposit Berpusat Muka (FCCCD). Struktur ANN terbaik dikenal pasti secara berasingan bagi setiap objektif. Model-model ini menunjukkan ketepatan tinggi dengan nilai R^2 sebanyak 0.9919 untuk penggunaan bahan, 0.9360 untuk kekuatan tegangan, dan 0.9558 untuk ketepatan dimensi. Model ANN ini kemudian digabungkan dengan algoritma Carian Organisma Simbiotik (SOS) yang dipertingkat melalui Strategi Kepelbagaian (DS), menghasilkan algorithma MOSOS-DS. Pengoptimuman berasaskan Pareto dan analisis jarak Euclidean menghasilkan solusi terbaik dengan penggunaan bahan sebanyak 4.41 g, kekuatan tegangan 37.76 Pa dan ketepatan dimensi 1.05 mm. Walaupun kaedah teras yang digunakan telah pun wujud, kajian ini membangunkan gabungan yang lebih mantap melalui penambahbaikan dan penyesuaian struktur model mengikut setiap tindak balas. Hasilnya ialah satu rangka kerja berskala yang membolehkan kawalan proses FDM secara lebih tepat dan berasaskan data dalam pembuatan tambahan.

Kata kuncis: Multi-objective optimisation (MOO), symbiotic organism search (SOS), fused deposition modelling (FDM), artificial neural network (ANN), diversification strategy

1.0 INTRODUCTION

Fused Deposition Modelling (FDM) is an additive manufacturing process that is currently gaining traction in both industrial and academic spheres for versatility and cost-effectiveness. This process involves a nozzle to deposit melted thermoplastic filament in a layer-wise manner, gradually forming intricate three-dimensional structures. FDM offers fine control over part shape, print parameters, and material properties, making it versatile for various demands. However, achieving consistent, high-quality prints is challenging due to the complexity of fine-tuning multiple parameters, prompting interest in optimisation algorithms to enhance print quality and efficiency [1], [2], [3]. The manufacturing industry aims to reduce costs while maintaining optimal functionality. Printers that minimize material consumption while ensuring high mechanical strength and dimensional accuracy are preferred. Studies show that adjusting parameters like layer height, infill density, printing speed, and temperature is key to achieving these goals in 3D printing [4], [5]. Conventional optimisation methods (heuristic algorithms), struggle with the complexities of multiple variables and managing conflicting objectives. However, non-conventional methods excel by expanding the search space and integrating domain-specific knowledge for more precise parameter optimisation [6]. Unconventional techniques frequently make use of embedded memory to preserve and enhance previously effective solutions, guaranteeing successful navigation out of constrained regions of the search space and successfully identifying ideal configurations [7]. Numerous studies have shown the effectiveness of advanced optimisation strategies. Metaheuristic algorithms in FDM optimisation enhance product quality and functionality, adjusting parameters systematically and proving robust across diverse additive manufacturing applications. [8], [9]. Optimisation for multiple outputs is often approached individually through single-objective optimisation that optimises each response independently. While effective, it does not address all objectives simultaneously. A better approach is multi-objective optimisation, which considers all outputs simultaneously with specified weights [10], [11]. Multi-objective optimisation entails identifying a set of solutions that are not dominated by any other solutions, as indicated by the Pareto front generated during the process [12]. Srivastava *et al*. [13] investigated this strategy to optimise the layout of a Fortus 250mc FDM printer. A response surface approach was employed alongside desirability analysis to investigate issues including build time, material and support volume reduction, and manufacturing costs, resulting in a balanced solution with good overall quality. Camposeco-Negrete [14] uses multi-objective optimisation along with the Taguchi method to achieve a mix of productivity, sustainability, quality, and structural performance. A desirability analysis was used to demonstrate how simultaneous optimisation enhances both efficiency and quality of printed products.

Previous research shows that combining multi-objective optimisation with various approaches can effectively optimise FDM process parameters. However, advanced optimisation algorithms may enhance outcomes further. The Symbiotic Organism Search (SOS) algorithm is notable for its use of three natural symbiotic relationships. First, mutualism involves organisms cooperating to improve solutions. Then, commensalism allows stronger organisms to benefit weaker ones without harm. Lastly, parasitism

encourages organisms to explore new search areas through random mutations [15]. According to Tran *et al*. [16], the SOS search technique entails breaking the search region up into smaller sections and employing the answers from each zone to gradually converge on the best options. Initially proposed by Tran *et al*. [17], MOSOS was used to optimise work shift use in construction projects, exceeding conventional and other unconventional methods such as Non-dominated Sorting Genetic Algorithm-II (NSGA-II) and Multi-Objective Particle Swarm Optimisation (MOPSO). This demonstrates MOSOS's ability to solve complicated issues by retaining solution variety while also identifying optimal process parameters for numerous objectives. Dash *et al*. [18] presented an improved SOS for optimising Distribution Static Synchronous Compensators (DSTACOMs) and Distributed Generation (DG) in electric networks. This version includes antagonistic learning and an adaptive chaotic local search strategy to reduce power loss, improve voltage profiles, and enhance stability. Results show significant improvements in managing trade-offs, outperforming traditional multi-objective optimisation methods. Subsequently, Baysal *et al*. [19] enhanced SOS with Non-Dominated Sorting Multi-Objective Symbiotic Organism Search (NSMOSOS) for feature selection in Brain-Computer Interface (BCI) systems. This method balances classification accuracy with feature count, achieving 97.86% accuracy with 11 features and 96.57% with 19 features. The study confirms NSMOSOS' superiority over other SOS variants in BCI applications.

Consequently, MOSOS has great potential in tackling multi-objective optimisation problems by utilising a fitness-sharing approach to direct convergence in the direction of the Pareto front while preserving population variety. While MOSOS alone can converge to good solutions, there is a possibility that it may suffer from premature convergence and become trapped in local optima [20]. Meanwhile, Differential Evolution (DE) is a population-based metaheuristic optimisation algorithm that uses a mutation operator and a crossover operator to evolve the population toward the optimal solution. Hybridizing MOSOS with DE combines the strengths of both algorithms and overcomes their weaknesses. Specifically, DE can provide diversification strategies to MOSOS, preventing premature convergence and enhancing the exploration of the search space. This synergy improves optimisation quality, addressing challenges like premature convergence and ensuring better exploration and convergence in complex domains like FDM.

Furthermore, traditional methods, such as linear regression, often struggle to capture the intricate, non-linear relationships between process parameters such as layer height, infill densities, printing speed, and temperature [21]. These limitations reveal the shortcomings of conventional modelling approaches, which can fail to adequately represent the complexity of FDM processes. To overcome these challenges, advanced techniques leveraging Artificial Intelligence (AI) have been employed. The integration of artificial intelligence (AI) into process modelling has demonstrated substantial improvements in predictive capabilities [22], [23]. Sai *et al*. [24] demonstrated the efficacy of ANFIS in modelling the FDM process and enhancing the surface quality of biomedical implants through integrated WOA and multi-objective optimisation, achieving reduced build time while maintaining compressive strength. Mishra *et al*. [25], combined RSM and ANFIS for modelling the FDM process and used multi-objective NSGA-II for optimisation. Their findings highlighted ANFIS's superior predictive capability and the effectiveness of combining AI-based models with multi-objective optimisation in FDM.

In this study, an integrated approach was performed between Artificial Neural Networks (ANN) modelling and multi-objective symbiotic organism search with diversification strategy (DS) to search to the optimal FDM process parameters to trade-off between material consumption, tensile strength, and dimensional accuracy. Using Response Surface Methodology - Face Centered Central Composite Design (RSM-FCCCD), the experimental design incorporates layer height, infill densities, printing speed, and printing temperature as input parameters. The optimum ANN model structure is found via network training with varied hidden layers and neurons. The integration of ANN with Multi-Objective Symbiotic Organism Search with Diversification Strategy (MOSOS-DS) enhances prediction accuracy and optimises processes in FDM. By identifying optimal trade-offs, this approach improves resource utilisation and market competitiveness. Its benefits extend beyond FDM to other manufacturing sectors with different parameters and objectives.

2.0 METHODOLOGY

The methods used to design, print, and analyze the specimens in this study are outlined as follows. The specimens were meticulously crafted using the Ender 3 V2, a robust open-source 3D printer known for its versatility and reliability in additive manufacturing, as illustrated in Figure 1 and detailed in Table 1. The specimens were manufactured per the stringent specifications of International Standard ISO/ASTM D638 Type IV, with precise dimensions documented in Figure 2. The printing material chosen for this investigation is polylactic acid plus (PLA+).

The experiment design (DOE) employed Response Surface Modelling (RSM) with a face-centered central composite design (FCCCD). The input parameters included critical variables such as layer height (LT), infill densities (ID), printing speed (PS), and printing temperature (PT). These parameters and their corresponding values are detailed in Table 2, providing a clear roadmap for the experimental setup. The selected parameter ranges were determined based on prior research [4–5], [26–30], manufacturer guidelines [31], printer capabilities, industry best

practices [32], and preliminary calibration tests tailored to this study's setup. The experimental setup utilised a single-block full factorial design, incorporating three factorial points, three axial points, and six centre points. In total, 78 experimental runs were conducted, comprising 72 runs at non-centre points and 6 runs at centre points, as outlined in Table 3. This design strategy ensured robustness in capturing the variability of the input factors and their impact on the output responses.

Figure 1 FDM 3D printer

Table 1 Specification for Ender 3 V2

Specification	Description
Close print chamber	No
Max extruder temperature	250 ℃
Max heated bed temperature	100 ℃
Nozzle size	0.4 *mm*
Build volume	220 × 220 × 250 *mm*
Layer height	0.1 – 0.4 *mm*

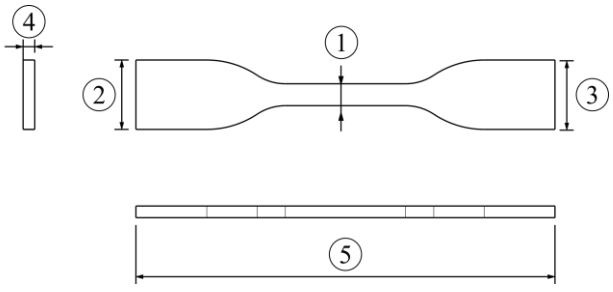

Figure 2 Dimension ISO/ASTM D638 Type IV

Table 2 Three levels of the four process parameters.

Process parameter	Unit	Level 1	Level 2	Level 3
Layer height (*LT*)	*mm*	0.2	0.26	0.32
Infill density (*ID*)	*%*	20	50	80
Printing speed (*PS*)	*mm/s*	50	100	150
Printing temperature (*PT*)	℃	185	200	215

Table 3 Experimental data

Run	Layer Height (mm)	Printing Speed (mm/s)	Infill Density (%)	Printing Temperature (℃)	Material Consumption (g)	Tensile Strength (Pa)	Dimensional Accuracy (mm)
1	0.32	100	50	200	5.23	42.32	0.27
2	0.26	100	50	200	5.03	35.72	0.30
3	0.20	150	80	215	5.86	37.24	0.36
4	0.26	100	20	200	4.44	32.64	0.31
5	0.20	50	80	215	5.65	36.89	0.28
6	0.32	50	80	185	5.56	44.80	0.23
7	0.32	50	20	215	4.88	37.11	0.30
8	0.20	150	20	185	3.94	31.50	0.23
9	0.32	100	50	200	5.24	39.93	0.29
10	0.32	50	20	215	4.91	37.21	0.28
11	0.32	150	80	215	5.60	45.90	0.40
12	0.20	150	80	215	5.68	42.02	0.35
13	0.26	100	50	200	5.11	36.94	0.30
14	0.20	50	20	185	3.98	31.44	0.25
15	0.32	100	50	200	5.25	41.05	0.29
16	0.20	150	80	185	5.67	38.67	0.28
17	0.26	100	50	185	5.07	37.85	0.25
18	0.26	100	50	200	5.16	38.58	0.31
19	0.20	50	20	215	3.99	30.36	0.29
20	0.26	150	50	200	5.08	36.13	0.32
21	0.20	150	20	215	3.97	29.46	0.35
22	0.26	100	50	200	5.10	36.36	0.30
23	0.20	150	80	185	5.60	40.11	0.29
24	0.20	150	20	215	3.93	29.14	0.37
25	0.32	50	80	185	5.47	41.40	0.26
26	0.32	150	80	215	5.58	42.89	0.39
27	0.32	150	20	215	4.74	37.40	0.38
28	0.20	150	20	215	3.91	29.04	0.35
29	0.26	100	20	200	4.36	33.19	0.27
30	0.26	100	50	215	5.16	36.93	0.34
31	0.26	100	80	200	5.84	43.25	0.33
32	0.32	150	20	215	4.86	38.30	0.37
33	0.32	50	80	215	5.59	43.88	0.27
34	0.32	50	20	185	4.82	42.06	0.23
35	0.26	100	50	185	5.08	33.51	0.28
36	0.32	150	20	185	4.66	39.16	0.26
37	0.26	100	80	200	5.82	40.68	0.33
38	0.20	50	80	185	5.62	37.96	0.24
39	0.32	150	80	215	5.58	43.37	0.38
40	0.20	50	80	215	5.86	39.16	0.26
41	0.32	150	80	185	5.47	46.71	0.30
42	0.32	50	20	185	4.78	42.99	0.22
43	0.20	100	50	200	4.87	35.60	0.25
44	0.26	100	50	200	5.18	39.40	0.27
45	0.32	50	80	185	5.67	44.27	0.24
46	0.20	100	50	200	4.85	32.90	0.26
47	0.26	100	20	200	4.44	35.50	0.27
48	0.32	50	20	215	4.92	40.82	0.27
49	0.20	50	80	185	5.71	40.64	0.24
50	0.26	100	50	200	5.14	40.47	0.29
51	0.32	150	20	185	4.64	40.55	0.28
52	0.20	50	80	215	5.70	40.05	0.27

Run	Layer Height (mm)	Printing Speed (mm/s)	Infill Density (%)	Printing Temperature (°C)	Material Consumption (g)	Tensile Strength (Pa)	Dimensional Accuracy (mm)
53	0.26	50	50	200	5.21	39.73	0.26
54	0.26	150	50	200	5.14	39.23	0.31
55	0.20	100	50	200	5.10	36.79	0.28
56	0.26	100	50	215	5.44	41.25	0.35
57	0.26	100	50	185	5.30	39.85	0.27
58	0.26	100	50	215	5.43	40.88	0.34
59	0.26	50	50	200	5.20	41.31	0.23
60	0.20	150	20	185	3.91	31.35	0.25
61	0.20	50	80	185	5.74	39.77	0.25
62	0.20	150	80	185	5.70	41.80	0.27
63	0.32	150	80	185	5.49	47.63	0.29
64	0.20	50	20	185	3.94	32.51	0.22
65	0.20	150	80	215	5.84	42.86	0.37
66	0.20	50	20	185	3.96	32.14	0.24
67	0.32	150	80	185	5.46	45.93	0.30
68	0.20	50	20	215	4.02	31.81	0.28
69	0.32	50	80	215	5.76	47.58	0.31
70	0.32	150	20	185	4.63	39.28	0.28
71	0.26	50	50	200	5.19	38.79	0.26
72	0.20	150	20	185	3.88	30.65	0.23
73	0.32	150	20	215	4.86	40.87	0.36
74	0.26	100	80	200	5.67	44.70	0.29
75	0.26	150	50	200	4.93	39.07	0.30
76	0.32	50	80	215	5.66	47.08	0.31
77	0.20	50	20	215	3.97	32.40	0.28
78	0.32	50	20	185	4.79	44.05	0.21

Artificial Neural Network (ANN) models are powerful tools used to analyze input data and make predictions by leveraging interconnected nodes, each with assigned weights [33]. The ANN architecture consists of an input layer, hidden layers, and an output layer. The input layer receives raw data, while the hidden layers learn the relationships among input variables. The output layer generates the final predictions to enable the model to make accurate forecasts.

The architecture of the ANN was carefully designed to balance model complexity with practical limitations in computation time and resources. Rather than relying on predefined structures from existing literature, an unbiased exploration of possible model architecture was conducted. Specifically, the number of hidden layers varied from 1 to 3, and the number of neurons per layer from 1 to 20. These limits were selected to allow sufficient architectural diversity while keeping training time manageable and avoiding overfitting. Before training, the data were standardized through normalization to eliminate biases from extreme values and large variances [34]. This step was crucial for improving the model's learning effectiveness. We also partitioned the data, using 70% for training, 15% for testing, and 15% for validation, to ensure the model generalizes well to new data [35], [36].

The performance of each ANN structure was rigorously evaluated using several metrics: R^2, Mean Squared Error (*MSE*), Root Mean Squared Error (*RMSE*), Mean Absolute Error (*MAE*), and Mean Absolute Percentage Error (*MAPE*). These metrics, which are widely recognized for assessing model performance, are presented in Eq. (3) through Eq. (7). Although some studies use only a subset of these indicators, all five were included in this work to ensure a thorough and unbiased evaluation. Given the large number of ANN configurations tested, and the minimal variation in their results, it was essential to evaluate models from multiple statistical perspectives. Metrics representing absolute and squared error, proportional deviation, and overall fit were collectively used to ensure an unbiased selection of the most accurate architecture. The final model was chosen based on its consistent performance across all five indicators.

By identifying the most suitable ANN structure, a predictive model was established to capture the relationship between input parameters and target responses. This trained network was then embedded within an optimising algorithm as a surrogate evaluator, enabling rapid performance estimation for candidate solutions during optimisation. With this integration, the computational load was significantly reduced, allowing the algorithm to effectively explore the solution space while maintaining predictive accuracy.

Building on this foundation, The MOSOS-DS (Multi-Objective Symbiotic Organisms Search with Diversification Strategy) was employed to enhance the original MOSOS algorithm by incorporating mutation and crossover mechanisms. These diversification strategies allow the algorithm to explore new regions of the search space and exploit existing solutions more effectively. MOSOS-DS is an improvement of MOSOS with better convergence to the Pareto front by enhancing exploration and exploitation capabilities. The optimisation results for MOSOS-DS will be compared to those of the original MOSOS to evaluate the improvements achieved.

A detailed illustration of the MOSOS-DS algorithm's process is shown in flowchart in Figure 3. The process begins by specifying problem parameters, including the objectives, decision variables, and algorithm settings, such as population size and maximum iterations. An initial population of solutions is generated, and an external repository is used to store non-dominated solutions throughout the optimisation. Each iteration of the MOSOS-DS (Multi-Objective Symbiotic Organisms Search with Diversification Strategy) algorithm involves three distinct phases: mutualism, commensalism, and parasitism. These phases are designed to iteratively improve the population of solutions through cooperation, interaction, and competition, while diversification strategies like mutation and crossover are employed to enhance exploration and exploitation of the search space.

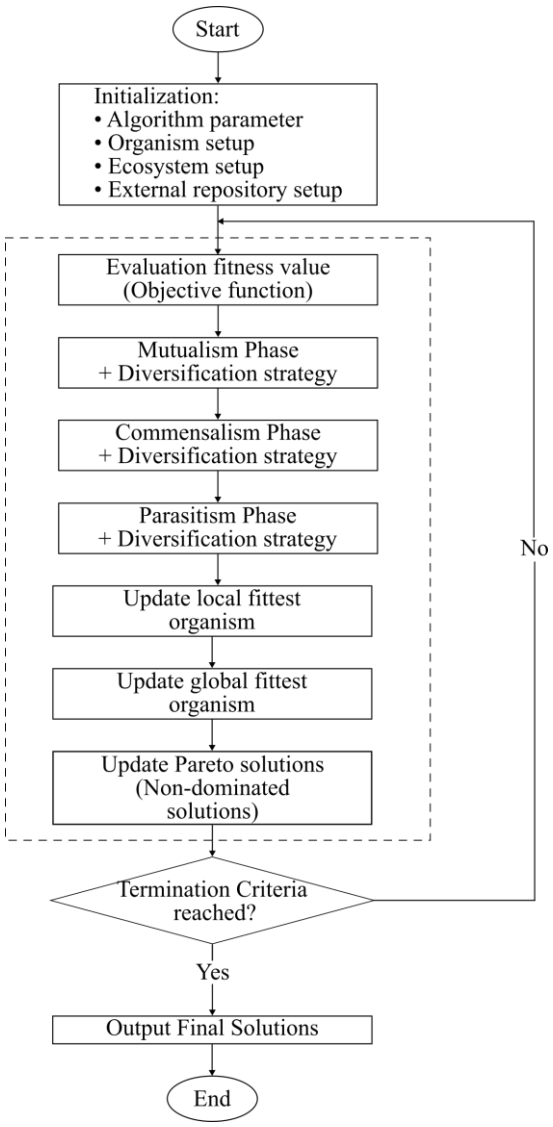

Figure 3 Flowchart of the MOSOS-DS algorithm

First, in the mutualism phase, two organisms, X_i and X_j, enhance each other's fitness by sharing traits, updating their solutions by combining their current values and the best solution. A new solution for X_i is generated by blending its state with contributions from a randomly selected organism, and the same applies for X_j. This cooperative process fosters a solution for space exploration. The diversification strategy introduces mutation, enhancing ecosystem variability and promoting exploration, followed by crossover to merge the mutated organism with the current ecosystem, increasing diversity. Then, in commensalism, one organism benefits without affecting the other. The i^{th} organism's new candidate solution is based on the difference between the best solution and the randomly selected organism, with no feedback from the latter. Diversification is applied to enhance variability. Lastly, in parasitism, a parasite vector P_i competes with a randomly selected organism X_j. If P_i has higher fitness, it replaces X_j in the ecosystem; otherwise, X_j gains immunity. This models parasitism, with the outcome based on fitness. Diversification is again applied.

After each phase, the domination process evaluates new solutions using Pareto dominance. A solution X_a dominates X_b if it is better in all objectives and superior in at least one. This process identifies superior solutions and guides the optimisation towards the Pareto-optimal front. At the end of each iteration, the non-dominated solutions are added to the repository, with less important ones removed if the repository is full. This process continues for a set number of iterations, after which the Pareto front is plotted to display the trade-offs between conflicting objectives. The diversification strategy allows the algorithm to avoid premature convergence and find a well-balanced set of solutions for multi-objective optimisation problems. For further details, refer to the pseudocode presented in Figure 4

MOSOS-DS were employed to determine the best process parameters for the fused deposition modelling (FDM) process, utilising ANN models for material consumption, tensile strength, and dimensional accuracy, as illustrated in Figure 5. The optimisation inputs are layer height (*LH*), infill densities (*ID*), printing speed (*PS*), and printing temperature (*PT*). We used three different ANN models to predict the responses for material consumption (*MC*), tensile strength (*TS*), and dimensional accuracy (*DA*). The algorithm then optimises these inputs to address all three responses until the maximum iteration is reached. The fitness value guides the optimisation process toward the Pareto front, resulting in several non-dominated optimal solutions with the best trade-offs obtained from the Pareto front. The solutions were then ranked by calculating the Euclidean distance.

```
Begin
Specify parameters for the process problems
Specify parameters for the MOSOS DS algorithm
Initialize population of organism in ecosystem
Initialize external repository

For each iteration do
    For each organism in the ecosystem do
        Select leader from the external repository
        Mutualism phase + diversification strategy
        Determine domination
        Commensalism phase + diversification strategy
        Determine domination
        Parasitism phase + diversification strategy
        Determine domination

        Determine best domination
    End for
    Update non-dominated organism to the external repository
End for
Plot Pareto chart
End
```

Figure 4 Pseudo code for MOSOS-DS

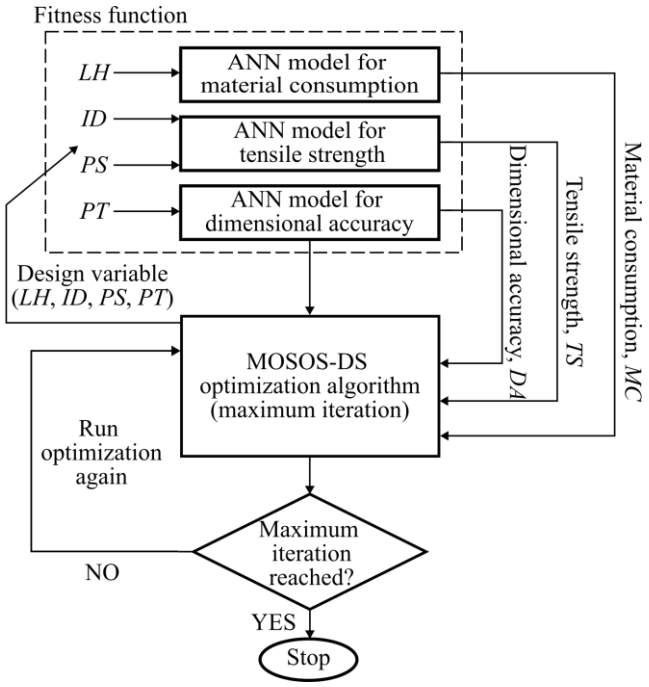

Figure 5 Integration of ANN with MOSOS-DS

3.0 RESULTS AND DISCUSSION

Three networks with varying hidden layers (single, double, and triple) were trained with up to 20 neurons each to find the best model. Each network was trained with a unique combination of neurons per layer, resulting in 20 structures for a single hidden layer, 210 structures for two hidden layers, and 1540 structures for three hidden layers. The final Artificial Neural Networks (ANN) models selected to predict material consumption, tensile strength, and dimensional accuracy are summarized in Table 4. Each structure was evaluated using five key performance metrics: *R², MSE, RMSE, MAE, and MAPE*. These metrics were calculated across training, validation, testing, and overall datasets. Retaining all five allowed a multidimensional assessment of model performance, which was especially important given the small differences observed among hundreds of candidate models.

The ANN model with the structure 4-19-14-1 was found to be the most effective for predicting material consumption. It achieved the highest R² values for both training and overall performance. It also recorded the lowest *RMSE, MSE, MAE*, and *MAPE* among all evaluated structures, indicating exceptional predictive accuracy and strong generalization. This performance confirms its reliability as the optimal model for this output.

In the case of tensile strength, the best-performing structure was 4-16-15-12-1, comprising three hidden layers with 16, 15, and 12 neurons, respectively. It provided the highest R² value during testing, which approached 1. Additionally, it recorded the lowest values for *RMSE, MSE, MAE*, and *MAPE* across the datasets, reinforcing its suitability for capturing complex, nonlinear relationships in the data.

For dimensional accuracy, two candidate structures of 4-12-11-11-1 and 4-9-1-1 showed comparable R² values (0.9558 and 0.9558). However, the 4-12-11-11-1 model was found to marginally outperform the 4-9-1-1 structure, demonstrating lower *MAE*, and *MAPE* (4.13 and 11.78%). *R²* alone could not distinguish between models with comparable correlation scores. This reinforces the need for multiple metrics to detect subtle yet significant variations in predictive performance. The inclusion of all five metrics allowed for more nuanced comparisons, ultimately supporting the selection of the most accurate ANN structures for each specific prediction objective.

Collectively, these findings highlight an important insight where adding more hidden layers and neurons may increase architectural diversity, but it does not guarantee better predictive performance. For example, in the case of material consumption, the more complex structure of 4-10-6-2-1 recorded a lower *R²* (0.9872 overall) and higher *MAE* (2.75) compared to simpler structures like 4-19-14-1, which achieved a higher *R²* (0.9919) and lower *MAE* (1.97). In addition to that, it is worth noting that a model that performs well for one objective may fall short for another. This reinforces a key principle that each response variable is shaped by different input relationships. Therefore, using separate, purpose-built models for each objective is essential to capture these differences and ensure reliable, balanced outcomes across all predictions.

Table 4 Performance function of structures for material consumption, tensile strength and dimensional accuracy

Structure	Function	Training	Validation	Testing	Overall
		Material consumption			
4-19-14-1	R^2	0.9959	0.9886	0.9895	0.9919
	MSE	0.0004	0.0030	0.0015	0.0010
	RMSE	0.0202	0.0546	0.0388	0.0310
	MAE	1.3912	3.7567	2.9446	1.9742
	MAPE	2.5999	7.2505	7.3304	3.9825
		Tensile strength			
4-16-15-12-1	R^2	0.9483	0.9439	0.9639	0.9360
	MSE	0.0034	0.0106	0.0089	0.0053
	RMSE	0.0582	0.1030	0.0942	0.0726
	MAE	4.6014	8.5412	8.3572	5.7372
	MAPE	10.2539	15.9038	17.9923	12.2144
		Dimensional accuracy			
4-12-12-11-1	R^2	0.9747	0.9444	0.8686	0.9558
	MSE	0.0538	0.0043	0.0075	0.0029
	RMSE	0.0410	0.0652	0.0867	0.0538
	MAE	7.0791	5.4463	7.0791	4.1263
	MAPE	8.2772	20.3342	19.9749	11.7818

Building upon the selection of the most reliable ANN structures for each response, the next phase of this study focuses on their integration within a multi-objective optimisation framework. These selected models serve as predictive engines within the Multi-Objective Symbiotic Organism Search with Diversification Strategy (MOSOS-DS) algorithm, enabling the exploration of trade-offs among material consumption, tensile strength, and dimensional accuracy under varying input parameters. A tailored fitness function is developed to standardize input parameters and assess their performance using these models. Initial ranges for input variables and settings for integrated ANN with MOSOS-DS are defined in Table 5 and Table 6 respectively. The performance of the MOSOS algorithm is largely governed by its parameter settings, which balance exploration and exploitation to effectively identify a diverse set of optimal solutions for FDM process optimisation. As shown in Table 6, all parameter values were adopted from established literature to ensure methodological consistency and credible benchmarking. These settings include four decision variables (layer height, printing speed, infill density, printing temperature), a maximum of 100 iterations, an ecosystem size of 200, and seven grids per dimension. Additionally, an inflation rate of 0.1 was applied, along with selection pressures for leader and deletion mechanisms ($\beta = 2$, $\gamma = 2$), as recommended in prior studies to promote convergence efficiency and solution diversity [17], [37–43]. The integrated approach of integrated ANN with MOSOS-DS ensures robust multi-objective optimisation, facilitating thorough exploration of the objective space. Visualization of results using Pareto fronts in three dimensions offers insights into trade-offs among material consumption, tensile strength, and dimensional accuracy. Ten solutions positioned nearest to the centroid of the MOSOS-DS Pareto front are highlighted as shown in Figure 6 as solutions with the most optimal compromises among the conflicting objectives. These ten selected solutions from MOSOS-DS will be compared to those from MOSOS to evaluate the effectiveness and improvements of the new algorithm.

Table 5 Range of parameters

Parameter	Lower bound	Upper bound
Layer height	0.2	0.32
Printing speed	50	150
Infill density	20	80
Printing temperature	185	215

Table 6 MOSOS-DS initial parameter setting [17], [37–43]

Parameter	Setting Value
Number of decision variables	4
Maximum number of iterations	100
Ecosystem size	200
Number of grids per dimension	7
Inflation rate	0.1
Leader Selection Pressure (beta)	2
Deletion Selection Pressure (gamma)	2

Table 7 and Table 8 show the Euclidean distance for MOSOS and MOSOS-DS where solution number 5 from Table 8 (MOSOS-DS) was proven to be the greatest solution with the best trade-off between the three objectives. Solution 5 MOSOS-DS comprises 0.23*mm* layer height (*LH*), 57.51% Infill density (*ID*), 51.74*mm/s* printing speed (*PS*), and 203.78℃ printing temperature (*PT*) resulting in 4.41*g* of material consumption (*MD*), 37.76*Pa* of tensile strength (*TS*) and 1.05*mm* dimensional accuracy (*DA*). Euclidean distance provides a numerical indicator of how well each solution fits the intended optimisation goals. By computing distances relative to an ideal reference point, it facilitates the identification of solutions that strike the optimal balance across multiple objectives, ensuring robust and reliable decision-making processes.

The efficacy of MOSOS-DS was compared to MOSOS using Euclidean distance to evaluate the trade-offs between the objectives. A Euclidean distance of 0.5 or less is considered the optimal trade-off among the objectives. The total Euclidean distance is then summed to identify the smallest total distance, representing the best overall optimisation that balances the objectives. Both approaches yield the same number of optimal solutions based on Euclidean distances of less than 0.5. However, the advantage of MOSOS-DS over MOSOS becomes evident in their total Euclidean distances, with MOSOS-DS achieving a shorter total distance of 5.4623 compared to 5.9653 for MOSOS. It also yielded the lowest individual distance of 0.1440 (Solution 5), compared to 0.3023 (Solution 3) for MOSOS, demonstrating its superior performance in simultaneously optimising all objectives. This confirms that MOSOS-DS achieved stronger convergence toward well-balanced solutions across the three objectives.

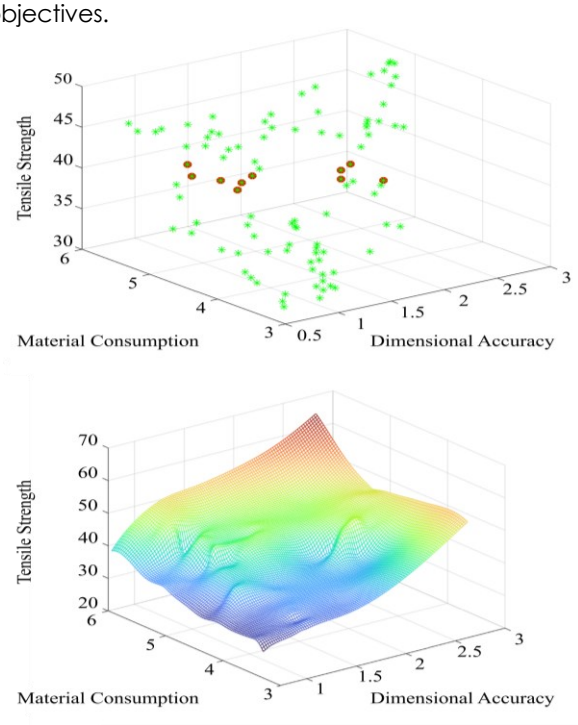

Figure 6 MOSOS-DS Pareto optimal results

Table 7 MOSOS Ranking of solutions

No.	Material consumption	Tensile strength	Dimensional accuracy	Euclidean Distance
1	0.7107	0.5878	0.0833	0.4751
2	1.0000	1.0000	0.8333	0.7817
3	0.3471	0.2994	0.6667	0.3023
4	0.8017	0.8812	0.9167	0.6403
5	0.2645	0.3842	0.9167	0.4924
6	0.3223	0.4950	0.7500	0.3068
7	0.0000	0.1257	1.0000	0.8000
8	0.0496	0.0000	0.9167	0.7915
9	0.3058	0.2066	0.9167	0.5454
10	0.0579	0.0070	0.0000	0.8298
Shortest Total Distance				5.9653
Best Solution				0.3023

Table 8 MOSOS-DS Ranking of solutions

No.	Material consumption	Tensile strength	Dimensional accuracy	Euclidean Distance
1	1.0000	1.0000	0.7692	0.7566
2	0.1146	0.0811	0.8462	0.6662
3	0.0000	0.1608	0.7692	0.6615
4	0.6354	0.7649	0.7692	0.4012
5	0.5729	0.4541	0.6154	0.1440
6	0.4896	0.2095	0.0000	0.5784
7	0.1771	0.0000	1.0000	0.7774
8	0.2083	0.2527	1.0000	0.6295
9	0.8646	0.3662	0.5385	0.3903
10	0.9375	0.5662	0.6154	0.4573
Shortest Total Distance				5.4623
Best Solution				0.1440

Experimental validation confirms the reliability of optimised solutions. While the optimisation process produces promising outcomes, conducting confirmation tests is essential to evaluate how well these solutions perform in real-world applications. Subjecting the selected solutions to experimental tests verifies whether they meet the objectives simulated during optimisation. Ten solutions, selected as per Figure 7, were 3D printed and tested for material consumption, tensile strength, and dimensional accuracy using standardized procedures and equipment. The results of these experimental tests are presented in Table 9, along with the calculated errors relative to the objectives simulated from the Pareto front. Each objective's calculated error is found to be less than 1, indicating that the optimisation process has achieved a high level of accuracy and reliability. Moreover, such low errors demonstrate that the optimisation algorithm effectively converges on solutions that accurately reflect the complexities of the fused deposition modelling (FDM) process, ensuring robust performance in real-world applications.

Collectively, these findings underscore the value of integrating ANN modelling method with bio-inspired optimisation for data-driven process control in FDM. The ANN-MOSOS-DS framework not only identified accurate predictive models but also enabled clear visualization of trade-offs through Pareto-based analysis. The success of experimental validation, with all percentage errors falling below 1%, further demonstrates the practical viability of the optimised solutions for real-world implementation.

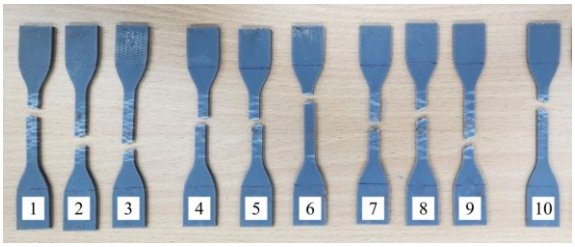

Figure 7 Specimen from the validation experiment

Table 9 Three objectives MOSOS-DS experimental confirmation results and error

Solution	Material Consumption		Tensile strength		Dimensional accuracy	
	Measured value (g)	Percentage error (%)	Measured value (Pa)	Percentage error (%)	Measured value (mm)	Percentage error (%)
1	5.60	0.05	44.19	0.15	0.14	0.86
2	4.75	0.05	37.39	0.05	0.15	0.87
3	4.64	0.05	37.98	0.07	0.14	0.89
4	5.25	0.15	42.45	0.11	0.14	0.87
5	5.19	0.18	40.14	0.06	0.12	0.89
6	5.11	0.11	38.34	0.05	0.04	0.98
7	4.81	0.06	36.78	0.08	0.17	0.92
8	4.84	0.06	38.66	0.02	0.17	0.92
9	5.47	0.28	39.50	0.00	0.11	0.95
10	5.54	0.33	40.98	0.07	0.12	0.94

4.0 CONCLUSION

This study demonstrates the powerful role of AI-driven modelling and multi-objective optimisation in improving Fused Deposition Modelling (FDM) processes. Critical parameters such as layer height, infill density, printing speed, and temperature were optimised to improve material usage, tensile strength, and dimensional accuracy. Artificial Neural Network (ANN) models were developed using experimental data from 78 PLA+ specimens and rigorously evaluated across multiple structures. The highest-performing architecture were 4-19-14-1 for material consumption with an R^2 value of 0.9919, 4-16-15-12-1 for tensile strength with R^2 of 0.9360, and 4-12-11-11-1 for dimensional accuracy with R^2 of 0.9558. These models were integrated into the Symbiotic Organism Search (SOS) algorithm, which was enhanced using a Diversification Strategy (DS) to form the improved Multi-Objective Symbiotic Organism Search with Diversification Strategy (MOSOS-DS) framework. When compared with the standard MOSOS approach, MOSOS-DS consistently produced superior Pareto-optimised solutions. It achieved a total Euclidean distance of 5.4623 and the lowest individual distance of 0.1440, reflecting better trade-off balancing.

Experimental validation confirmed prediction errors below 1% for all ten solutions generated by MOSOS-DS. Among them, Solution 5 emerged as the best compromise. It achieved 4.41 g of material usage, 37.76 Pa of tensile strength, and 1.05 mm of dimensional accuracy. These outcomes were obtained using a 0.23 mm layer height, 57.51% infill density, 51.74 mm/s printing speed, and 203.78 °C printing temperature. These results confirm that integrating accurate ANN structures with MOSOS-DS provides not only reliability, but also a scalable and intelligent optimisation strategy that can be applied to other complex manufacturing processes.

Acknowledgement

This research was funded by the Ministry of Education Malaysia through Fundamental Research Grant Scheme No. FRGS/1/2020/ICT02/UNIMAP/02/1 and supported by the researchers from University Malaysia Perlis. The authors would like to express their gratitude to the University Malaysia Perlis for their guidance in completing this research study.

Conflicts of Interest

The authors declare that there is no conflict of interest regarding the publication of this paper.

References

[1] Waseem, M., T. Habib, U. Ghani, M. Abas, Q. M. U. Jan, and M. A. Z. Khan. 2022. Optimisation of Tensile and Compressive Behaviour of PLA 3D Printed Parts Using Categorical Response Surface Methodology. *International Journal of Industrial and Systems Engineering.* 41(4): 417–437. https://doi.org/10.1504/IJISE.2022.124997.

[2] Vorkapić, M., I. Mladenović, M. Pergal, T. Ivanov, and M. Baltić. 2022. Optimisation of Tensile Stress of Poly(lactic Acid) 3D Printed Materials Using Response Surface Methodology. *Tribology and Materials.* 1(2): 70–80. https://doi.org/10.46793/tribomat.2022.009.

[3] Myers, D., A. Abdel-Wahab, F. Hafeez, N. Kovacev, and K. Essa. 2022. Optimisation of the Additive Manufacturing Parameters of Polylactic Acid (PLA) Cellular Structures for Biomedical Applications. *Journal of the Mechanical Behavior of Biomedical Materials.* 136(December). https://doi.org/10.1016/J.JMBBM.2022.105447.

[4] Johansson, F. 2016. Optimizing Fused Filament Fabrication 3D Printing for Durability: Tensile Properties and Layer Bonding. Master's thesis, Blekinge Institute of Technology, Karlskrona, Sweden.

[5] Nguyen, V. H., T. N. Huynh, T. P. Nguyen, and T. T. Tran. 2020. Single and Multi-Objective Optimisation of Processing Parameters for Fused Deposition Modelling in 3D Printing Technology. *International Journal of Automotive and Mechanical Engineering.* 17(1): 7542–7551. https://doi.org/10.15282/IJAME.17.1.2020.03.0558.

[6] Kumar, M., and P. Khatak. 2017. An Investigation of Conventional and Non-Conventional Optimization Techniques in CNC Machining. *International Journal of Advance Scientific Research and Engineering Trends.* 2(6).

[7] Fávero, L. P., and P. Belfiore. 2019. Integer Programming. In *Data Science for Business and Decision Making*. 887–918. https://doi.org/10.1016/B978-0-12-811216-8.00019-7.

[8] Goudswaard, M., A. Nassehi, and B. Hicks. 2019. Automation and Intelligent Manufacturing." https://doi.org/10.1016/j.promfg.2020.01.049.

[9] Fountas, N. A., I. Papantoniou, J. D. Kechagias, D. E. Manolakos, and N. M. Vaxevanidis. 2022. Modeling and Optimization of Flexural Properties of FDM-Processed PET-G Specimens Using RSM and GWO Algorithm. *Engineering Failure Analysis.* 138: 106340. https://doi.org/10.1016/J.ENGFAILANAL.2022.106340.

[10] Limleamthong, P., and G. Guillén-Gosálbez. 2018. Combined Use of Bilevel Programming and Multi-objective Optimization for Rigorous Analysis of Pareto Fronts in Sustainability Studies: Application to the Redesign of the UK Electricity Mix. *Computer Aided Chemical Engineering.* 43: 1099–1104. https://doi.org/10.1016/B978-0-444-64235-6.50192-3.

[11] De Buck, V., P. Nimmegeers, I. Hashem, C. A. Muñoz López, and J. Van Impe. 2021. Exploiting Trade-Off Criteria to Improve the Efficiency of Genetic Multi-Objective Optimisation Algorithms. *Frontiers in Chemical Engineering.* 3: 3. https://doi.org/10.3389/FCENG.2021.582123.

[12] Fox, A. D., D. W. Corne, C. G. Mayorga Adame, J. A. Polton, L. A. Henry, and J. M. Roberts. 2019. An Efficient Multi-Objective Optimization Method for Use in the Design of Marine Protected Area Networks. *Frontiers in Marine Science.* 6(February): 17. https://doi.org/10.3389/FMARS.2019.00017.

[13] Srivastava, M., S. Maheshwari, T. Kundra, and S. Rathee. 2017. Multi-Response Optimization of Fused Deposition Modelling Process Parameters of ABS Using Response Surface Methodology (RSM)-Based Desirability Analysis. *Materials Today: Proceedings.* 4(2): 1972–1977. https://doi.org/10.1016/J.MATPR.2017.02.043.

[14] Camposeco-Negrete, C. 2020. Optimization of Printing Parameters in Fused Deposition Modeling for Improving Part Quality and Process Sustainability. *The International Journal of Advanced Manufacturing Technology.* 108: 2131–2147.

[15] Ezugwu, A. E., O. J. Adeleke, and S. Viriri. 2018. Symbiotic Organisms Search Algorithm for the Unrelated Parallel Machines Scheduling with Sequence-Dependent Setup Times. *PLoS One.* 13(7): e0200030. https://doi.org/10.1371/JOURNAL.PONE.0200030.

[16] Tran, D. H., M. Y. Cheng, and D. Prayogo. 2016. A Novel Multiple Objective Symbiotic Organisms Search (MOSOS) for Time–Cost–Labor Utilization Tradeoff Problem. *Knowledge-Based Systems.* 94(February): 132–145. https://doi.org/10.1016/J.KNOSYS.2015.11.016.

[17] Tran, D. H., L. Luong-Duc, M. T. Duong, T. N. Le, and A. D. Pham. 2018. Opposition Multiple Objective Symbiotic Organisms Search (OMOSOS) for Time, Cost, Quality and Work Continuity Tradeoff in Repetitive Projects. *Journal of Computational Design and Engineering.* 5(2): 160–172. https://doi.org/10.1016/J.JCDE.2017.11.008.

[18] Dash, S. K., S. Mishra, U. Raut, and A. Y. Abdelaziz. 2021. An Improved Symbiotic Organisms Search Algorithm for Multi-Objective Simultaneous Optimal Allocation of DSTATCOM and DG Units. In *2021 International Conference in Advances in Power, Signal, and Information Technology (APSIT 2021)*. https://doi.org/10.1109/APSIT52773.2021.9641337.

[19] Baysal, Y. A., S. Ketenci, I. H. Altas, and T. Kayikcioglu. 2021. Multi-Objective Symbiotic Organism Search Algorithm for Optimal Feature Selection in Brain Computer Interfaces. *Expert Systems with Applications.* 165(March): 113907. https://doi.org/10.1016/J.ESWA.2020.113907.

[20] Grandis, H., and Sungkono. 2022. Modified Symbiotic Organisms Search (SOS) Algorithm for Controlled-Source Audio-Frequency Magnetotellurics (CSAMT) One-Dimensional (1D) Modelling. *Journal of Earth System Science.* 131(1). https://doi.org/10.1007/S12040-021-01808-7.

[21] Mohamed, O. A., S. H. Masood, and J. L. Bhowmik. 2016. Mathematical Modeling and FDM Process Parameters

Optimization Using Response Surface Methodology Based on Q-Optimal Design. *Applied Mathematical Modelling*. 40(23–24): 10052–10073. https://doi.org/10.1016/J.APM.2016.06.055.

[22] Mohamed, O. A., S. H. Masood, and J. L. Bhowmik. 2021. Modeling, Analysis, and Optimization of Dimensional Accuracy of FDM-Fabricated Parts Using Definitive Screening Design and Deep Learning Feedforward Artificial Neural Network. *Advances in Manufacturing*. 9(1): 115–129. https://doi.org/10.1007/s40436-020-00336-9.

[23] Lyu, J., and S. Manoochehri. 2019. Dimensional Prediction for FDM Machines Using Artificial Neural Network and Support Vector Regression. In *Proceedings of the ASME Design Engineering Technical Conference*,. Vol. 1. https://doi.org/10.1115/DETC2019-97963.

[24] Sai, T., V. K. Pathak, and A. K. Srivastava. 2020. Modeling and Optimization of Fused Deposition Modeling (FDM) Process through Printing PLA Implants Using Adaptive Neuro-Fuzzy Inference System (ANFIS) Model and Whale Optimization Algorithm. *Journal of the Brazilian Society of Mechanical Sciences and Engineering*. 42(12): 1–19. https://doi.org/10.1007/S40430-020-02699-3.

[25] Mishra, P., S. Sood, V. Bharadwaj, A. Aggarwal, and P. Khanna. 2023. Parametric Modeling and Optimization of Dimensional Error and Surface Roughness of Fused Deposition Modeling Printed Polyethylene Terephthalate Glycol Parts. *Polymers*. 15(3): 546. https://doi.org/10.3390/POLYM15030546.

[26] Deshwal, S., A. Kumar, and D. Chhabra. 2020. Exercising Hybrid Statistical Tools GA-RSM, GA-ANN and GA-ANFIS to Optimize FDM Process Parameters for Tensile Strength Improvement. *CIRP Journal of Manufacturing Science and Technology*. 31(November): 189–199. https://doi.org/10.1016/j.cirpj.2020.05.009.

[27] Dev, S., and R. Srivastava. 2020. Experimental Investigation and Optimization of FDM Process Parameters for Material and Mechanical Strength. *Materials Today: Proceedings*. 26: 1995–1999. https://doi.org/10.1016/j.matpr.2020.02.435.

[28] Buj-Corral, I., A. Bagheri, A. Domínguez-Fernández, and R. Casado-López. 2019. Influence of Infill and Nozzle Diameter on Porosity of FDM Printed Parts with Rectilinear Grid Pattern. *Procedia Manufacturing*. 41: 288–295. https://doi.org/10.1016/j.promfg.2019.09.011.

[29] Hodzic, D., and A. Pandzic. 2021. Influence of Infill Design on Compressive and Flexural Mechanical Properties of FDM Printed PLA Material. *Annals of DAAAM & Proceedings*. 191–200.

[30] Alsoufi, M. S., M. W. Alhazmi, D. K. Suker, W. K. Hafiz, S. S. Almalki, and R. O. Malibari. 2019. Influence of Multi-Level Printing Process Parameters on 3D Printed Parts in Fused Deposition Molding of Poly(lactic) Acid Plus: A Comprehensive Investigation. *American Journal of Mechanical Engineering*. 7(2): 87–106. https://doi.org/10.12691/ajme-7-2-5.

[31] SUNLU. 2023. SUNLU PLA & PLA Plus 3D Filaments, 1kg/2.2lbs. Fit Most of FDM Printers. Accessed February 26, 2023. https://www.sunlu.com/products/pla-pla-plus-3d-filaments-1kg-2-2lbs-fit-most-of-fdm-printer.

[32] Buj-Corral, I., A. Tejo-Otero, and F. Fenollosa-Artés. 2021. "Use of FDM Technology in Healthcare Applications: Recent Advances." In *Fused Deposition Modeling Based 3D Printing*, 277–297. https://doi.org/10.1007/978-3-030-68024-4_15.

[33] Bin Ashoor, B., A. Giwa, and S. W. Hasan. 2019. Full-Scale Membrane Distillation Systems and Performance Improvement Through Modeling: A Review. In *Current Trends and Future Developments on (Bio-)Membranes: Membrane Desalination Systems: The Next Generation*. 105–140. https://doi.org/10.1016/B978-0-12-813551-8.00005-X.

[34] Puig-Arnavat, M., and J. C. Bruno. 2015. Artificial Neural Networks for Thermochemical Conversion of Biomass. In *Recent Advances in Thermochemical Conversion of Biomass*. 133–156. https://doi.org/10.1016/B978-0-444-63289-0.00005-3.

[35] Ng, N. Y. Z., R. H. Abdul Haq, O. M. F. Marwah, F. H. Ho, and S. Adzila. 2022. Optimization of Polyvinyl Alcohol (PVA) Support Parameters for Fused Deposition Modelling (FDM) by Using Design of Experiments (DOE). *Materials Today: Proceedings*. 57: 1226–1234. https://doi.org/10.1016/J.MATPR.2021.11.046.

[36] Shirmohammadi, M., S. J. Goushchi, and P. M. Keshtiban. 2021. Optimization of 3D Printing Process Parameters to Minimize Surface Roughness with Hybrid Artificial Neural Network Model and Particle Swarm Algorithm. *Progress in Additive Manufacturing*. 6(2): 199–215. https://doi.org/10.1007/s40964-021-00166-6.

[37] Sedighizadeh, M., M. Esmaili, and A. Eisapour-Moarref. 2017. Hybrid Symbiotic Organisms Search for Optimal Fuzzified Joint Reconfiguration and Capacitor Placement in Electric Distribution Systems. *INAE Letters*. 2(3): 107–121. https://doi.org/10.1007/s41403-017-0029-5.

[38] Yuejun, A. L. 2024. New Search Strategy for Multi-Objective Evolutionary Algorithm. *Heliyon*. 10(24): e40917. https://doi.org/10.1016/j.heliyon.2024.e40917.

[39] Saha, S., and V. Mukherjee. 2019. A Novel Multiobjective Chaotic Symbiotic Organisms Search Algorithm to Solve Optimal DG Allocation Problem in Radial Distribution System. *International Transactions on Electrical Energy Systems*. 29(5): e2839. https://doi.org/10.1002/2050-7038.2839.

[40] Kotb, R., A. M. Ewais, and A. M. Hemeida. 2019. Single and Multi-Objective Optimization Algorithms. *International Journal of Applied Energy Systems*. 1(2): 77–84. https://doi.org/10.21608/ijaes.2019.169954.

[41] Banihashemi, S. A., and M. Khalilzadeh. 2022. A Robust Bi-Objective Optimization Model for Resource Levelling Project Scheduling Problem with Discounted Cash Flows. *KSCE Journal of Civil Engineering*. 26(6): 2539–2554. https://doi.org/10.1007/s12205-022-0679-z.

[42] Shao, J., Y. Lu, Y. Sun, and L. Zhao. 2025. An Improved Multi-Objective Particle Swarm Optimization Algorithm for the Design of Foundation Pit of Rail Transit Upper Cover Project. *Scientific Reports*. 15(1): 10403. https://doi.org/10.1038/s41598-025-87350-8.

[43] Yang, D., K. Redmill, and U. Ozguner. 2020. A Multi-State Social Force Based Framework for Vehicle-Pedestrian Interaction in Uncontrolled Pedestrian Crossing Scenarios. In *Proceedings of the IEEE Intelligent Vehicles Symposium*. 1807–1812. https://doi.org/10.1109/IV47402.2020.9304561.